

Hydrophobic bioadhesive composites for human motion detection

Singh, Manisha; Solic, Ivan; Steele, Terry W. J.

2021

Singh, M., Solic, I. & Steele, T. W. J. (2021). Hydrophobic bioadhesive composites for human motion detection. *ACS Macro Letters*, 10(11), 1353-1358.

<https://dx.doi.org/10.1021/acsmacrolett.1c00559>

<https://hdl.handle.net/10356/158570>

<https://doi.org/10.1021/acsmacrolett.1c00559>

This document is the Accepted Manuscript version of a Published Work that appeared in final form in *ACS Macro Letters*, copyright © American Chemical Society after peer review and technical editing by the publisher. To access the final edited and published work see <https://doi.org/10.1021/acsmacrolett.1c00559>.

Downloaded on 10 Dec 2023 17:47:35 SGT

1 **Hydrophobic bioadhesive composites for human motion detection**

2 Manisha Singh^{1,2}, Ivan Solic², Terry W. J. Steele^{1,2*}

3 ¹NTU-Northwestern Institute for Nanomedicine (NNIN), Interdisciplinary Graduate School
4 (IGS), Nanyang Technological University (NTU), Singapore 637553

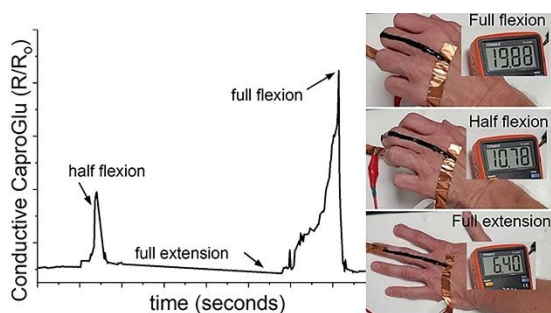
5 ²School of Materials Science and Engineering (MSE), Nanyang Technological University
6 (NTU), Singapore 639798

7 *Correspondence to Terry W. J. Steele (e-mail: wjsteele@ntu.edu.sg)

8 **Abstract**

9 Conductive hydrogels are rapidly rising as sensing materials for bioelectronics applications
10 but lack mechanical and adhesion strength due to their excess water content. We propose a
11 diazirine-grafted polycaprolactone adhesive (aka CaproGlu)/carbon nanotubes (CNTs)
12 composite that can provide wet adhesion and strong mechanical properties at the tissue-
13 machine interface. The introduced CNTs not only reinforced the CaproGlu but also formed
14 electrically conducting pathways. The CaproGlu composites exhibited conductivity of 0.1 S
15 m^{-1} and charge storage capacity of $5 \mu\text{C cm}^{-2}$. The resulting composites are biocompatible
16 and can be used as strain sensors to detect mechanical deformations.

17 **for Table of Contents use only**



19

20 **Introduction**

21 Conductive hydrogels provide impressive biocompatibility and conformability for various
22 biomedical applications such as biosensing, implant interfacing, and wearable electronics¹⁻².
23 These applications require the interfacing biomaterials to be stretchable and easy to adhere to
24 highly complex and curvilinear tissues (e.g., skin, heart, etc.)³. Fragile and weak mechanical/
25 adhesion properties of hydrogels constitute an obstacle to their long-term applicability.
26 Moreover, because of their hydrophilic nature, hydrogels can potentially swell excessively,
27 and the increased water content can further compromise their mechanical properties^{1,4}.
28 Recent attempts of toughening the hydrogels involved the incorporation of conductive fillers
29 (e.g., silver, or gold nanowires)⁴. These fillers improved their mechanical and electrical
30 properties but showed negligible improvement in their adhesive characteristics. As a result,
31 hydrogels are unable to form stable interconnect patterns in hydrated conditions and require
32 complicated fixation methods, such as perfluoropolyether (PFPE), for their fabrication into
33 electrodes⁵. The development of interface materials that can adhere to soft tissues, mimic
34 tissue mechanical properties, has electrical conductivity, and cyclic flexibility to
35 accommodate repetitive body movements are needed for bioelectronic and sensing
36 applications.

37 CaproGlu is a novel synthetic bioadhesive that transitions from liquid to a viscoelastic bio
38 rubber upon application of ultraviolet (UV) light dose⁶. In CaproGlu, a photocurable
39 crosslinker (aryl-diazirine) is grafted onto the surface of polycaprolactone (PCLT) polymer.
40 Diazirine is an initiator-free covalent crosslinker that is relatively stable under ambient
41 conditions but can be activated via voltage, heat, or UV⁷⁻¹³. In a more recent study, diazirine-
42 based materials have also been shown to crosslink under visible light (445 nm)¹⁴. However,
43 activation at 445 nm only occurs in presence of a catalyst and is reported to be stable in
44 absence of one. Diazirine grafted PCLT (aka CaproGlu) allows fine-tuning of mechanical and

45 adhesion properties via carbene insertion chemistry. CaproGlu is hydrophobic, exhibits
46 strong wet adhesion, withstands gamma irradiation sterilization, and is biocompatible^{6, 15}.
47 However, endowing the CaproGlu with good conductivity while maintaining mechanical and
48 adhesion strength is still challenging. Herein, carbon nanotubes (CNTs) are introduced into
49 CaproGlu at varying weight percentages following the percolation theory, forming CaproGlu
50 composites. The CNTs are hypothesized to provide a three-dimensional electron transfer
51 network throughout the non-conductive CaproGlu matrix. CNTs are chosen because of their
52 high electrical conductivity, high charge injection ability, and low mass density¹⁶. Diazirines
53 have been reported in the literature to functionalize CNTs for sensing and coating
54 applications¹⁷⁻¹⁸. Owing to the hydrophobic interactions between CaproGlu and CNTs, these
55 CaproGlu composites are anticipated to provide better dispersion of CNTs than those in
56 water. This work presents preliminary data on the influence of CNT additives on the
57 mechanical, adhesion, and electrical properties of CaproGlu. The CaproGlu composites are
58 also tested for strain sensing capabilities and successfully exhibited the potential for human
59 motion detection.

60 **Experimental Section**

61 **Preparation of CaproGlu composites**

62 CaproGlu bioadhesives with ~50% diazirine conjugation were synthesized as per the method
63 published previously⁶ and detailed synthesis steps are reported in the supplementary
64 information. The NC7000TM multi-walled carbon nanotubes (CNT) were purchased from
65 NANOCYL[®] (Belgium) in powder form. The technical details of the CNTs, as provided by
66 the supplier, are also available in the supplementary information. Different weight
67 percentages of 0.1-3% of multi-walled carbon nanotubes (CNT) additives were physically
68 mixed into the CaproGlu. The resulting composites with mixed CNTs and CaproGlu are

69 referred to as ‘CaproGlu composites’ throughout this manuscript. The composites were UV-
70 cured with an intensity of 250 mW cm⁻² for 60 seconds to obtain the viscoelastic films.

71 **Measurement of conductivity**

72 A two-point probe setup was used for the measurement of the resistance of the CaproGlu
73 composites. A concentric ring geometry was used, and a constant voltage of 1 V was supplied
74 using the Keithley 2450 Sourcemeter and the current was recorded. A voltage of 1V is chosen
75 to avoid the electrochemical activation (~1.5V) of diazirine¹⁹. The recorded current was then
76 used to calculate the resistance as per Ohm’s law. The relationship between surface resistivity
77 (ρ) and the surface resistance (R) for a concentric ring probe geometry was calculated by
78 ASTM D257-14 method, $\rho = R \times \frac{2\pi}{\ln\left(\frac{R2}{R1}\right)}$ where, R1 is the outer radius (1.5 mm) of the center
79 electrode, and R2 is the inner radius (2 mm) of the outer ring electrode. Since the composite
80 films are thin (~0.5 mm), then the volume resistivity is assumed equal to the surface
81 resistivity multiplied by the thickness.

82 **Characterization of mechanical properties**

83 A rheometer MCR 102 (Anton Paar) was used to measure the real-time oscillatory
84 rheological properties and tack adhesion. UV curing @ 365 nm was performed at an intensity
85 of 250 mW cm⁻². The following rheological parameters were used — frequency: 1 Hz, Shear
86 strain: 1%, gap: 0.2 mm, Probe PP10 (stainless steel). For the tack adhesion test, the samples
87 were pre-sheared for 1 s at a shear rate of 1 1/s, and then the probe was moved up at a
88 velocity of 50 μ m/s.

89 **Electrochemical characterization**

90 Electrochemical characterizations were performed with a three-electrode configuration using
91 a Potentiostat (Metrohm Autolab, The Netherlands) with a built-in frequency-response

92 analyzer. For impedance measurements, a voltage of 10 mV (RMS) was used, and the
93 complex impedance was measured using a sinusoidal input voltage over a range of
94 frequencies from 10^5 to 0.1 Hz. For cyclic voltammetry (CV), CaproGlu composites were
95 coated on the working electrode of area 0.071 cm^2 . CV measurements were conducted at a
96 scan rate of 100 mV s^{-1} in a potential window of -0.6 to 0.8 V vs. Ag/AgCl reference
97 electrode in phosphate-buffered saline (PBS) solution.

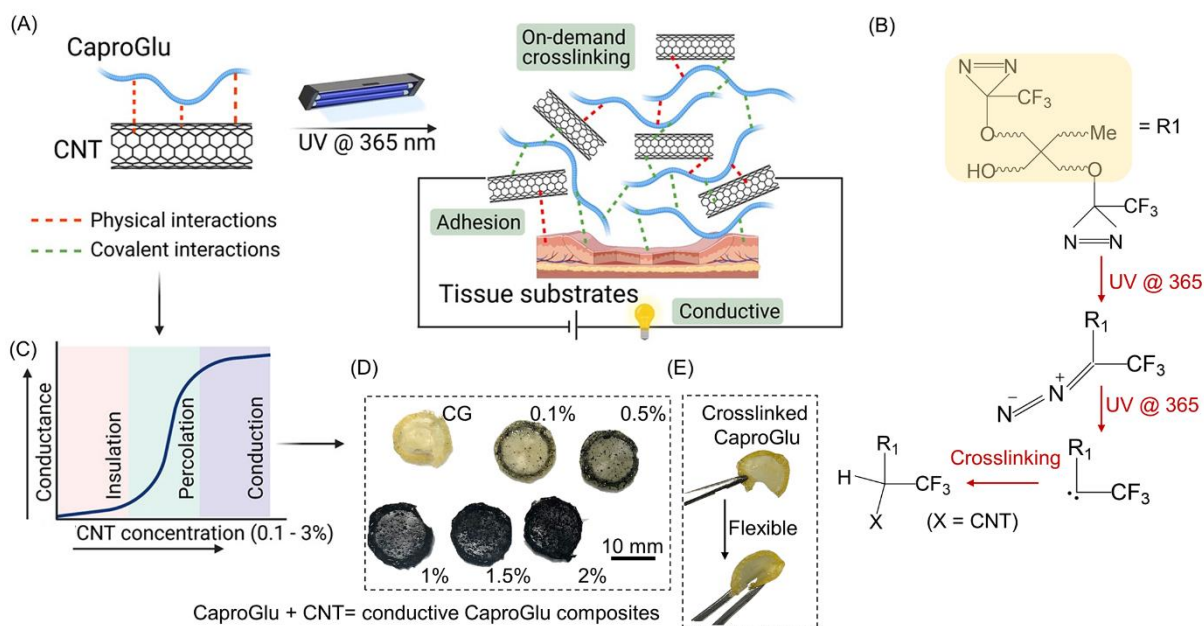
98 **Results and Discussion**

99 **Scope and study design**

100 CaproGlu has previously been reported to adhere to wet tissues with on-demand covalent
101 crosslinking⁶. The hydrophobic nature and tissue-mimicking properties of CaproGlu make it
102 a strong candidate for human-machine interfacing and sensing applications, but CaproGlu
103 lacks electrical conductivity. Herein, carbon nanotubes are physically mixed into CaproGlu
104 bioadhesives at varying weight percentages of 0.1-3% as per the percolation theory (**Figure**
105 **1**). High dynamic viscosity ($\sim 7 \text{ Pa}\cdot\text{s}$) of CaproGlu and hydrophobic interactions within the
106 composite may also allow for fair dispersion of CNTs in the CaproGlu (**Figure S1** and
107 **Figure S2**). Liquid CaproGlu composites turn into thin viscoelastic films by UV-curing via
108 carbene-mediated insertion chemistry (**Figure 1B-1E**). We evaluate the mechanical,
109 adhesive, and electrical structure-activity relationships at varying CNT concentrations via
110 real-time UV rheology, tack test, and two-point probe method, respectively. The sensitivity of
111 the CaproGlu composites against the detection of various mechanical deformations is also
112 studied.

113

114



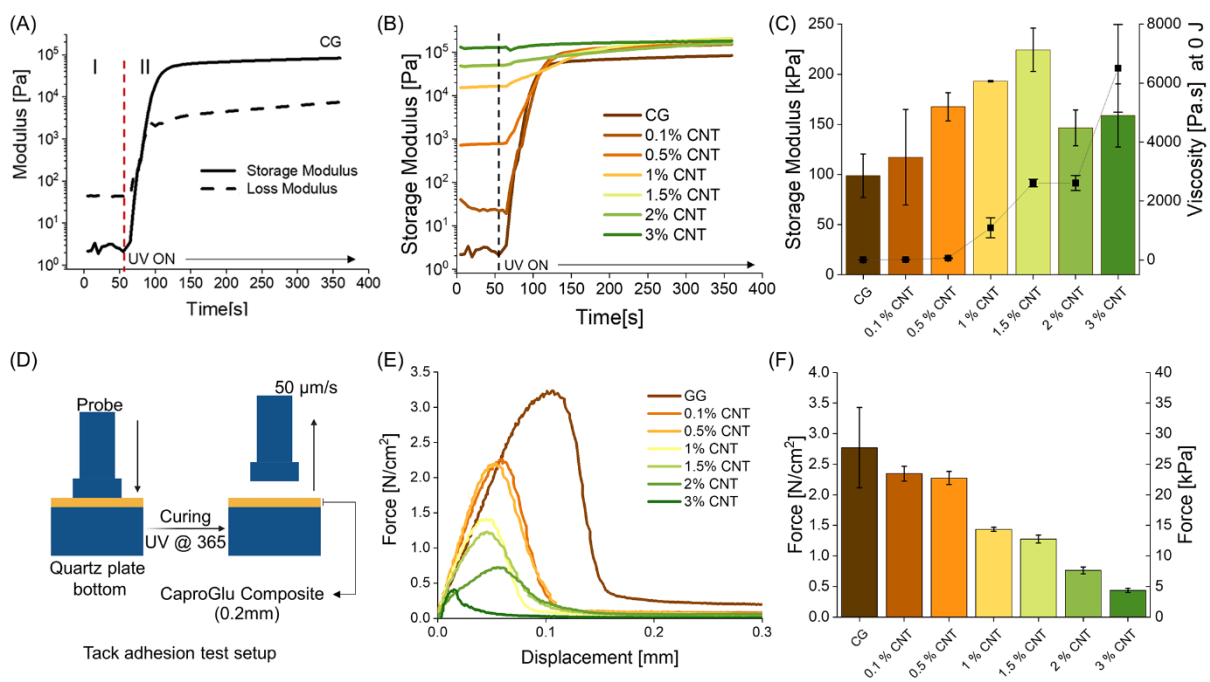
115

116 **Figure 1:** Overall Scheme and study design. A) Multi-walled carbon nanotubes (CNT) are
 117 physically mixed into CaproGlu (CG). CaproGlu can undergo a transition from liquid to
 118 viscoelastic solid (bio rubber) upon exposure to UV light. B) The crosslinking mechanism of
 119 CaproGlu under UV stimulation. A carbene intermediate performs as the active crosslinker
 120 and crosslinks with primary amines, sulfhydryls, carboxylic acid, and carboxyls groups
 121 available on the soft tissues. C) CaproGlu composites are prepared at a varying concentration
 122 of CNTs (0.1-3 wt %) as per the percolation theory. D) Thin viscoelastic films of the
 123 composites are obtained upon UV-mediated crosslinking. E) Crosslinked films are compliant
 124 and flexible.

125 **Mechanical and adhesion properties are optimized at ~1.5% CNT**

126 Real-time rheology assesses the viscoelastic properties of the CaproGlu composites upon UV
 127 exposure. The storage (G') and loss (G'') moduli are recorded against time for control CG
 128 samples (i.e., pristine CaproGlu). Before UV application, $G'' > G'$ shows that CaproGlu is a
 129 viscous fluid (**Figure 2A**). Upon UV activation, G' starts to rise rapidly, demonstrating a
 130 transition to viscoelastic solid. The rheological parameters were recorded for all the

131 formulations of the composites, and storage modulus (G') was seen to be rapidly increasing
 132 with UV light activation (**Figure 2B, Figure S3**). Before UV onset, the storage modulus of
 133 the composites is higher than the control CG, which could suggest a uniform dispersion of
 134 CNTs in the matrix. Storage modulus (G') after 5 minutes of UV dose increased to 225 kPa
 135 for 1.5% CNT concentration, which is ~ 2.3 -folds to that of the control CG (**Figure 2C**). The
 136 G' lies in the range of 100-250 kPa, which is similar to the mechanical modulus of various
 137 soft tissues (e.g., arteries, skin, heart, etc.)²⁰. Once the UV is turned off, the mechanical
 138 properties (G') of the cured CaproGlu composites stabilize within 20-30 seconds (**Figure**
 139 **S4**). The G' was seen to be decreasing as the amount of CNTs was increased to 2 wt % or
 140 higher. This could be attributed to the absorption of UV light by CNTs, leaving insufficient
 141 energy for diazirine activation. For CNT additives of 2 wt % or higher, thermal curing (~ 105
 142 $^{\circ}\text{C}$) can be opted to avoid partial curing via UV (**Figure S5**). The viscosity of the composites
 143 lies in the range of 10-7000 Pa.s, similar to that needed for extrusion printing of
 144 biomaterials²¹⁻²². This confirms the direct printability of the CaproGlu composites for the
 145 fabrication of various conductive circuits.



146

147 **Figure 2:** Evaluation of mechanical properties. A) Real-time rheological parameters (G' , G'')
148 for CaproGlu (CG) control. B) Comparison of real-time stimuli-based oscillatory rheology
149 (G') for CaproGlu composites. C) Storage modulus after 5 minutes of UV-mediated curing
150 (bar plots); dynamic viscosity of the CaproGlu composites before curing (scatter plots). D)
151 Set up of tack test. E) Representative force vs. displacement plots as a function of varying
152 CNT concentration (thickness 0.2 mm). F) Comparison of maximum tack adhesion strength.

153

154 Tack test measures the adhesion strength of the composites — mimicking the tensile forces
155 acting in the human body (**Figure 2D**). The representative load vs. displacement curves
156 demonstrate elastic behavior with reducing yield strength as the amount of CNTs is increased
157 from 0.1% to 3% (**Figure 2E**). For 1.5 % CNTs, the composites reached a maximum strain of
158 around 300% (thickness 0.2 mm). Compared with control CG, the maximum adhesion
159 strength of 1.5% CNT is reduced to half (**Figure 2F**). This is ascribed to the reduction of
160 diazirine (covalent crosslinker) in the composites as the amount of CNTs increases.
161 Depending on the concentration of CNT, the adhesion strength obtained is in the range of 5-
162 30 kPa. The adhesion strength could also be tuned by varying its covalent crosslinker
163 conjugation. Higher conjugation corresponds to higher adhesion strength⁶.

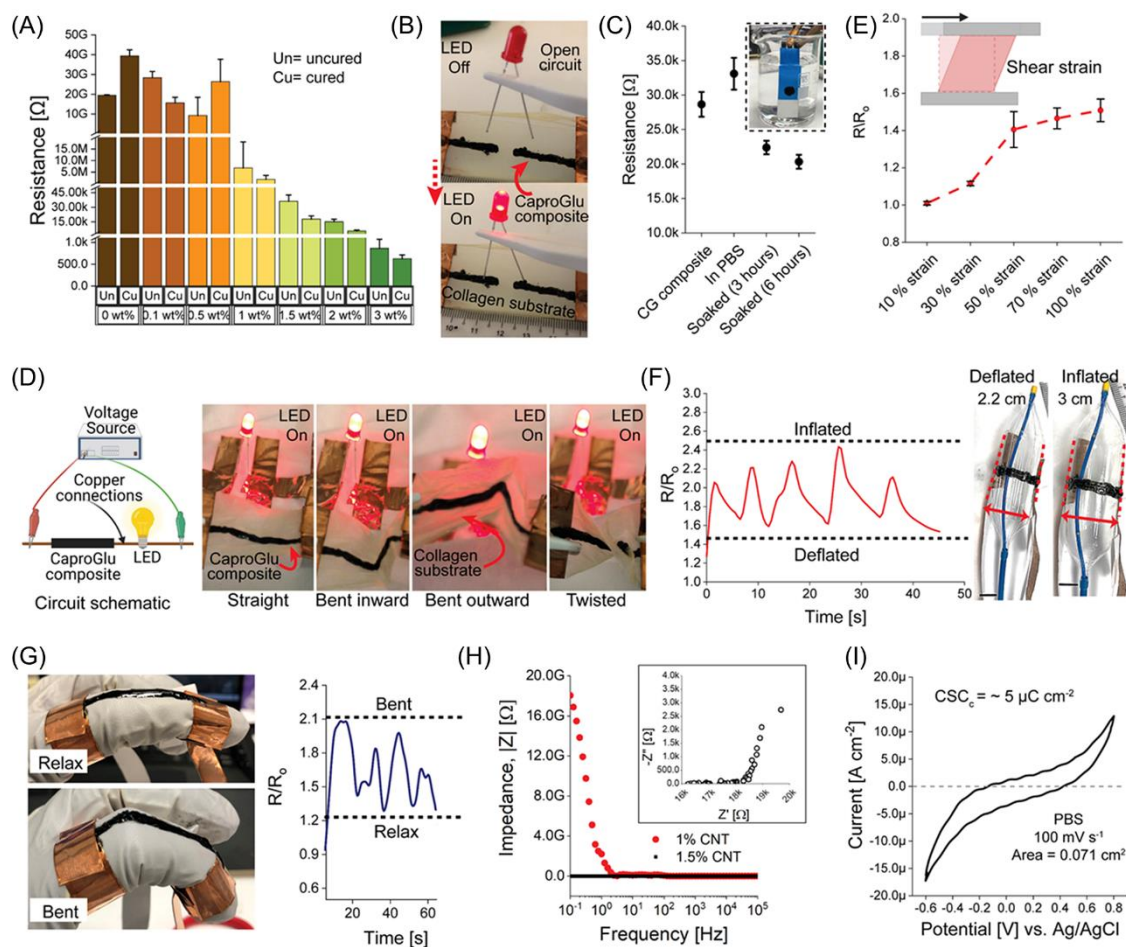
164 **Electrical properties and strain sensing**

165 As measured by the two-point probe method, the conductivity of the CaproGlu composites
166 can be tuned between 6 nS m^{-1} to 0.1 S m^{-1} . This is comparable to the electrical conductivity
167 of the soft tissues ($0.1\text{-}1.6 \text{ S m}^{-1}$)²³, suggesting that the CaproGlu composites can potentially
168 be employed as electrical adhesives at the human-machine bioelectronic interfaces.
169 Percolation is achieved at a CNT concentration of 1% (**Figure 3A**). The resistance of UV-
170 cured composites is lower as compared to uncured counterparts for CNT concentration

171 beyond 1% (**Figure 3A**). The transition of composites from liquid to viscoelastic solid could
172 result in an increasing percolation probability because of the tunneling through the
173 diazirine/diazoalkanes¹⁹. The desired conductivity and optimum concentration of the
174 conductive additives are cautiously considered based on the percolation transition. As a
175 result, there is a tradeoff between the electrical and mechanical properties of the composites.
176 Comparing the rheological, adhesion, and electrical data (**Figure 2**), the concentration of
177 CNTs is best optimized at 1.5%. The conductivity of 1.5% CNTs reached about 22×10^5
178 folds higher than that of CG control exhibiting an insulator-to-conductor transition. An
179 illustration of the conductivity of the CaproGlu composites is shown in **Figure 3B**, where a
180 straight electric circuit was hand-painted over a flexible collagen substrate to power a LED
181 (**Video S1**). To test conductivity under the isotonic physiological conditions, the composites
182 were soaked in PBS for 6 hours. A two-point probe measures the resistance and shows that
183 the conductivity of the soaked CaproGlu composites increases by ~33 % (**Figure 3C**). This
184 may be attributed to the permeation of the H^+ , OH^- ions into the porous composites. We also
185 anticipate that the hydrophobic nature of the composites would provide longer stability under
186 hydrated conditions than that of hydrogels, hence potentially improving the lifespan of the
187 implants/sensors.

188 The applicability of the composites for bioelectronic applications requires that the circuits
189 maintain their electrical conductivity under physiologically relevant strains (e.g., bending,
190 tension, shearing, etc.). To test this, the electric patterns of composites were hand-painted
191 over flexible collagen substrates and connected in a circuit with LED (**Figure 3D**). The
192 circuits when twisted and bent – both inward and outward, preserved the continuity as
193 indicated by the bright LED. The LED remained on and maintained the brightness despite
194 being deformed multiple times. To test the quantitative changes in the electrical
195 conductivity, the resistances were recorded under conditions of shear, tensile, and bending

196 strains (**Figure 3E- 3G**). CaproGlu's resistance (R) is measured under physiological strains
197 and normalized with respect to initial resistance (R_0). We observed an increase in the
198 resistance ($\sim 55\%$) as the shear strain was increased to 100% (**Figure 3E**). To measure the
199 applicability of the CaproGlu composites for strain sensing and human motion detection, we
200 performed cyclic mechanical deformations and recorded the resistance. For strain sensing, a
201 thin electric circuit was hand-painted over the balloon of an Edwards transfemoral balloon
202 catheter (**Figure 3F**). The balloon was inflated and deflated repeatedly exhibiting a strain of
203 $\sim 36\%$. The CaproGlu composites-based strain sensors were also hand-painted over the
204 forefinger and crosslinked using UV light @ 365 nm (**Figure 3G**). After the applied
205 mechanical deformations in both the balloon and forefinger, the strain sensors reacted to the
206 motions rapidly. The change in resistance during balloon (inflation/deflation) or finger
207 (bent/relaxed) motions indicated a similar behavior where every peak corresponds to a
208 cycling of the balloon/finger motion. The variation in the resistance observed was up to ~ 65
209 % and $\sim 54\%$ for deformations in the balloon and finger, respectively. We observed no signs
210 of breakage indicating an electrical discontinuity in the circuits. The increase in the resistance
211 during the mechanical deformations is attributed to the stretching of the conductive networks
212 of CNTs in the CaproGlu composites.



213

214 **Figure 3:** Electrical and electrochemical characterizations. A) Comparison of resistance
 215 measured by the two-point probe method. B) LED connected in a circuit made up of
 216 CaproGlu composites illustrating electrical conductivity. C) Influence on the electrical
 217 conductivity upon incubation in phosphate-buffered saline (physiologically relevant isotonic
 218 conditions) for up to 6 hours. D) Illustration of electrical continuity in the electric circuits
 219 hand-painted using CaproGlu composites during multiple cycles of bending or twisting. E)
 220 Influence on conductivity under shear strains. F) Influence on conductivity under tensile
 221 strains showing composites' ability to sense the mechanical deformations. G) Effect on
 222 conductivity during bending movements. H) Impedance spectroscopy of composites vs.
 223 control CG. I) Electrochemical characterization of composites via cyclic voltammetry.

224 The applicability of the composites at the human-machine bioelectronic interface for
225 stimulation and recording requires electrochemical characterization via electrical impedance
226 spectroscopy (EIS) and cyclic voltammetry (CV). EIS investigations show that the impedance
227 reduction at low frequencies is significant in the case of 1.5% composites than that of 1%
228 CNT (**Figure 3H**). The almost vertical tail in Nyquist plots of 1.5% CNTs at low frequencies
229 shows the capacitive behavior of the CaproGlu composites (**Figure 3H, inset**). The
230 composites also exhibit 25 % lower impedance in the physiologically relevant frequency
231 range of 10^2 - 10^5 Hz. CV evaluates the charge transfer capacity (CSC) of the CaproGlu
232 composites at the interface. CSC estimates the number of charges that can be injected during
233 a tissue stimulation and is calculated by taking the integral of the cathodic current. The
234 assessed CSC is $5 \mu\text{C cm}^{-2}$, which is comparable to that of metallic electrodes (1 - $50 \mu\text{C cm}^{-2}$)²⁴⁻²⁵.
235

236 In conclusion, we have demonstrated a liquid, conductive polymer composite that can be
237 rapidly transitioned into a conductive bio-rubber, and still be bioadhesive. We are not aware
238 of any other biocompatible, shelf-stable, conductive liquid polymers that have this ability and
239 can also withstand gamma irradiation sterilization. Untreated carbon allotropes, e.g., CNTs,
240 can be directly dissolved in the liquid CaproGlu base which is a contrast to all hydrogel
241 formulations that require surface-functionalized CNT. The carbene-chemistry involved in
242 CaproGlu is one of the only known methods in literature to covalently react with carbon
243 nanotube surfaces under ambient conditions. The prepared composites can successfully
244 identify the small strains for human motion detection. The sensing capabilities demonstrated
245 in this work can also be expanded to applications such as electronic skin, wearable
246 electronics, and electrode coatings for tissue recording or stimulation. The preliminary data
247 warrant future work on bioelectronic and electroceutical applications.

248

249 Acknowledgments

250 This work was supported by the Ministry of Education Tier 2 Grant (MOE2018-T2-2-114):
251 CaproGlu, Double-sided wet-tissue adhesives, NTUitive POC (Gap) Fund NGF/2018/05:
252 Aesthetic Applications of CaproGlu Bioadhesives, and A*Star IAF PP Grant
253 (H19/01/a0/0II9): CathoGlu Bioadhesives-preventing catheter extravasation and skin
254 infections. Figures, videos, and digital illustrations are created with Adobe Illustrator, Adobe
255 Photoshop, BioRender, Adobe Premiere Pro, and Blender. The data is plotted and evaluated
256 with OriginPro 2019 software.

257 Conflict of interest

258 The authors declare no conflict of interest.

259 References

- 260 1. Green, R. A.; Hassarati, R. T.; Goding, J. A.; Baek, S.; Lovell, N. H.; Martens, P. J.; Poole-
261 Warren, L. A., Conductive hydrogels: mechanically robust hybrids for use as biomaterials.
262 *Macromolecular bioscience* **2012**, *12* (4), 494-501.
- 263 2. Liang, S.; Zhang, Y.; Wang, H.; Xu, Z.; Chen, J.; Bao, R.; Tan, B.; Cui, Y.; Fan, G.; Wang, W.,
264 Paintable and rapidly bondable conductive hydrogels as therapeutic cardiac patches. *Advanced*
265 *Materials* **2018**, *30* (23), 1704235.
- 266 3. Karunakaran, C.; Bhargava, K.; Benjamin, R., *Biosensors and bioelectronics*. Elsevier: 2015.
- 267 4. Tang, L.; Wu, S.; Qu, J.; Gong, L.; Tang, J., A Review of Conductive Hydrogel Used in Flexible
268 Strain Sensor. *Materials* **2020**, *13* (18), 3947.
- 269 5. Wang, Y.; Zhu, C.; Pfattner, R.; Yan, H.; Jin, L.; Chen, S.; Molina-Lopez, F.; Lissel, F.; Liu, J.;
270 Rabiah, N. I., A highly stretchable, transparent, and conductive polymer. *Science advances* **2017**, *3*
271 (3), e1602076.
- 272 6. Djordjevic, I.; Pokholenko, O.; Shah, A. H.; Wicaksono, G.; Blancafort, L.; Hanna, J. V.; Page, S.
273 J.; Nanda, H. S.; Ong, C. B.; Chung, S. R.; Chin, A. Y. H.; McGrouther, D.; Choudhury, M. M.; Li, F.; Teo,
274 J. S.; Lee, L. S.; Steele, T. W. J., CaproGlu: Multifunctional tissue adhesive platform. *Biomaterials*
275 **2020**, *260*, 120215.
- 276 7. Singh, M.; Yin, C. S.; Page, S. J.; Liu, Y.; Wicaksono, G.; Pujar, R.; Choudhary, S. K.; Kulkarni, G.
277 U.; Chen, J.; Hanna, J. V.; Webster, R. D.; Steele, T. W. J., Synergistic Voltaglue Adhesive Mechanisms
278 with Alternating Electric Fields. *Chemistry of Materials* **2020**, *32* (6), 2440-2449.
- 279 8. Singh, M.; Nanda, H. S.; Lee, J. Y. H.; Wang, J. K.; Tan, N. S.; Steele, T. W. J., Photocurable
280 platelet rich plasma bioadhesives. *Acta Biomaterialia* **2020**, *117*, 133-141.
- 281 9. Singh, M.; Webster, R. D.; J. Steele, T. W., Voltaglue Electroceutical Adhesive Patches for
282 Localized Voltage Stimulation. *ACS Applied Bio Materials* **2019**, *2* (6), 2633-2642.
- 283 10. Gan, L.; Tan, N. C. S.; Gupta, A.; Singh, M.; Pokholenko, O.; Ghosh, A.; Zhang, Z.; Li, S.; Steele,
284 T. W. J., Self curing and voltage activated catechol adhesives. *Chem Commun (Camb)* **2019**, *55* (68),
285 10076-10079.

- 286 11. Singh, M.; Nanda, H. S.; O'Rourke, R. D.; Jakus, A. E.; Shah, A. H.; Shah, R. N.; Webster, R. D.;
287 Steele, T. W. J., Voltalglue Bioadhesives Energized with Interdigitated 3D-Graphene Electrodes. *Adv*
288 *Healthc Mater* **2018**, *7* (21), e1800538.
- 289 12. Nanda, H. S.; Singh, M.; Steele, T. W. J., Thrombogenic Responses from Electro cured Tissue
290 Adhesives. *ECS Transactions* **2017**, *77* (11), 547-555.
- 291 13. Singh, M.; Varela, C. E.; Whyte, W.; Horvath, M. A.; Tan, N. C. S.; Ong, C. B.; Liang, P.;
292 Schermerhorn, M. L.; Roche, E. T.; Steele, T. W. J., Minimally invasive electroceutical catheter for
293 endoluminal defect sealing. *Science Advances* **2021**, *7* (14), eabf6855.
- 294 14. Djordjevic, I.; Wicaksono, G.; Šolić, I.; Singh, J.; Kaku, T. S.; Lim, S.; Ang, E. W. J.; Blancafort,
295 L.; Steele, T. W. J., Rapid Activation of Diazirine Biomaterials with the Blue Light Photocatalyst. *ACS*
296 *Applied Materials & Interfaces* **2021**, *13* (31), 36839-36848.
- 297 15. Djordjevic, I.; Wicaksono, G.; Solic, I.; Steele, T. W. J., In Vitro Biocompatibility of Diazirine-
298 Grafted Biomaterials. *Macromolecular Rapid Communications* **2020**, *41* (21), 2000235.
- 299 16. Endo, M.; Iijima, S.; Dresselhaus, M. S., *Carbon nanotubes*. Elsevier: 2013.
- 300 17. Lawrence, E. J.; Wildgoose, G. G.; Aldous, L.; Wu, Y. A.; Warner, J. H.; Compton, R. G.;
301 McNaughter, P. D., 3-Aryl-3-(trifluoromethyl)diazirines as Versatile Photoactivated "Linker"
302 Molecules for the Improved Covalent Modification of Graphitic and Carbon Nanotube Surfaces.
303 *Chemistry of Materials* **2011**, *23* (16), 3740-3751.
- 304 18. Hosu, O.; Elouarzaki, K.; Gorgy, K.; Cristea, C.; Sandulescu, R.; Marks, R. S.; Cosnier, S.,
305 Nanostructured photoactivatable electrode surface based on pyrene diazirine. *Electrochemistry*
306 *Communications* **2017**, *80*, 5-8.
- 307 19. Ping, J.; Gao, F.; Chen, J. L.; Webster, R. D.; Steele, T. W., Adhesive curing through low-
308 voltage activation. *Nat Commun* **2015**, *6*, 8050.
- 309 20. Saraf, H.; Ramesh, K.; Lennon, A.; Merkle, A.; Roberts, J., Mechanical properties of soft
310 human tissues under dynamic loading. *Journal of biomechanics* **2007**, *40* (9), 1960-1967.
- 311 21. Cui, X.; Li, J.; Hartanto, Y.; Durham, M.; Tang, J.; Zhang, H.; Hooper, G.; Lim, K.; Woodfield, T.,
312 Advances in Extrusion 3D Bioprinting: A Focus on Multicomponent Hydrogel-Based Biinks.
313 *Advanced healthcare materials* **2020**, *9* (15), 1901648.
- 314 22. Wu, Q.; Therriault, D.; Heuzey, M.-C., Processing and properties of chitosan Inks for 3D
315 printing of hydrogel microstructures. *ACS Biomaterials Science & Engineering* **2018**, *4* (7), 2643-2652.
- 316 23. Gabriel, C.; Peyman, A.; Grant, E. H., Electrical conductivity of tissue at frequencies below 1
317 MHz. *Physics in Medicine and Biology* **2009**, *54* (16), 4863-4878.
- 318 24. Dössel, O.; Schlegel, W. C., *World Congress on Medical Physics and Biomedical Engineering*
319 *September 7-12, 2009 Munich, Germany: Vol. 25/IX Neuroengineering, Neural Systems,*
320 *Rehabilitation and Prosthetics*. Springer Science & Business Media: 2010; Vol. 25.
- 321 25. Cogan, S. F., Neural stimulation and recording electrodes. *Annual review of biomedical*
322 *engineering* **2008**, *10*, 275-309.

323

324